Composition Dependence of the Interaction Parameter in Isotopic Polymer Blends

J. D. Londono,* A. H. Narten,† and G. D. Wignall

Oak Ridge National Laboratory, Oak Ridge, Tennessee 37831

K. G. Honnell, E. T. Hsieh, and T. W. Johnson

Research and Development, Phillips Petroleum Company, Bartlesville, Oklahoma 74004

F. S. Bates

Department of Chemical Engineering and Materials Science, University of Minnesota, Minneapolis, Minnesota 55455

Received November 11, 1993; Revised Manuscript Received February 22, 1994®

ABSTRACT: Isotopic polymer mixtures lack the structural asymmetries and specific interactions encountered in blends of chemically distinct species. In this respect, they form ideal model systems for exploring the limitations of the widely-used Flory–Huggins (FH) lattice model and for testing and improving new theories of polymer thermodynamics. The FH interaction parameter between deuterium-labeled and unlabeled segments of the same species (χ_{HD}) should in principle be independent of concentration (ϕ), though previous small-angle neutron scattering (SANS) experiments have shown that it exhibits a *minimum* at $\phi \sim 0.5$ for poly(vinylethylene) (PVE) and poly(ethylethylene) (PEE). We report new data on polyethylene (PE) as a function of molecular weight, temperature (T), and ϕ, which show qualitatively similar behavior. However, measurements on $\chi_{HD}(\phi)$ for polystyrene (PS) show a *maximum* at $\phi \sim 0.5$, in contrast to PVE, PEE, and PE. Reproducing the concentration dependence of ϕ in different model isotopic systems should serve as a sensitive test of the way in which theories of polymer thermodynamics can account for the details of the local packing and also the effects of noncombinatorial entropy, which appear to be the main cause of the variation of $\chi_{HD}(\phi)$ for PE. These data also serve to quantify the effects of isotopic substitution in SANS experiments on polyolefin blends and thus lay the groundwork for definitive studies of the compatibility of branched and linear polyethylenes.

Introduction

For over 2 decades, small-angle neutron scattering (SANS) has been used to yield information on the conformation and solubility of polymers via deuterium labeling. This provides a way of enhancing the natural scattering contrast between the components of a blend and relies on the propitious and substantial difference in the coherent scattering lengths of deuterium (D) and hydrogen (H). The discovery[1-3] of a small ($\sim 10^{-4}$), positive interaction parameter (χ_{HD}) between D-labeled and unlabeled monomers of the same polymer species has delineated the circumstances under which deuterium-labeling methods may be used in polymer science,[4] without unduly perturbing the system under investigation. Moreover, such mixtures form ideal model systems for improving existing theories of polymer thermodynamics (for example, by correcting[1,5-10] FH theory to account for the observed composition dependence of χ) or for developing new theories such as the polymer reference interaction site model[11] (PRISM). Isotopic blends lack the complications which arise from structural asymmetries and specific interactions, normally encounterd in blends of chemically distinct species, and χ_{HD} can be calculated to a good approximation from first principles.[12-14] Experiments[15] and simulations[16] on the molecular weight scaling behavior of model isotopic systems have ruled out PRISM theory as initially formulated, though a new closure approximation which exhibits the correct scaling behavior has recently been developed.[17]

SANS data[1] have shown that for poly(vinylethylene) (PVE) and poly(ethylethylene) (PEE) χ_{HD} increases sharply at the two composition extremes, hence displaying a parabolic upward behavior. Muthukumar[1] and Sariban and Binder[18] have discussed theoretical and simulation results in which a similar concentration dependence was observed. A parabolic upward behavior has also been reported in a recent study on model polyolefin blends[19] by SANS, although these results included interspecies interactions in addition to residual isotopic effects. The results of PRISM integral equation calculations reported by Schweizer and Yethiraj,[20] for the case of symmetric blends, also show a parabolic upward behavior, the curvature of which was dependent on the proximity to T_c. For nonsymmetric blends the predicted behavior depends on the structural and energetic asymmetries. Banaszak et al.[10] applied the lattice cluster theory (LCT) of Freed and co-workers[7-9] to the set of experimental SANS data of Krishnamoorti et al.[19] A parabolic downward dependence of χ on ϕ was reported, in disagreement with the experimental work. For other systems, LCT has been shown to predict[7,9] a variety of functional dependencies.

In this paper, we report an extensive set of measurements on polyethylene (PE), as a function of molecular weight (MW), temperature (T), and concentration (volume fraction, ϕ). Also, previous data[2] have been repeated and extended to give the composition dependence of χ_{HD} for atactic polystyrene (PS). In both systems χ_{HD} is observed to vary linearly with inverse temperature, and for PE, our results show a *parabolic upward* composition dependence, as observed previously for PVE and PEE.[1] Moreover, for PE, both, χ_{HD} and the curvature of the observed composition dependence, decrease as a function of chain length (N). In contrast, our results for PS show a significant *parabolic downward* behavior of χ_{HD} with concentration with virtually no MW dependence. A similar functional behavior has also been reported in the work by Schwahn

† Deceased.

® Abstract published in *Advance ACS Abstracts*, April 1, 1994.

0024-9297/94/2227-2864$04.50/0

Table 1. Polyethylene Sample Details

N_D	M_w/M_n	N_N	M_w/M_n	ϕ_D	$B \times 10^4$	A (K)
2464	1.11	2538	1.1	0.221	−0.012	0.132
3275	1.10	3308	1.1	0.087	2.761	0.069
				0.457	0.242	0.089
4148	1.11	4598	1.1	0.044	1.628	0.325
				0.087	0.759	0.138
				0.131	0.808	0.100
				0.221	−0.907	0.139
				0.457	−0.843	0.127
				0.708	−0.859	0.133
5240	1.14	5200	1.1	0.087	0.121	0.142
				0.221	−1.193	0.146
				0.457	−1.434	0.147
				0.708	−0.936	0.128
6238	1.14	6630	1.1	0.087	0.428	0.116
				0.176	−0.690	0.132
7580	1.14	7700	1.1	0.087	−1.703	0.186

and co-workers[21] for PS isotopic blends, though, for $\phi_D < 0.2$ and $\phi_D > 0.8$, negative values of the interaction parameter were reported. The rich behavior reported in this work for the dependence of χ_{HD} in these two systems cannot be explained via FH theory and provides a challenge to current and future theoretical developments.

In addition, these experimental results throw light on SANS studies of the state of mixing in blends of linear and branched polyethylenes. Such systems have attained widespread commercial applications, though understanding the mechanical and melt-flow properties of the blends is handicapped by the absence of a consensus at the most fundamental level, i.e., the degree of mixing of the components both in the melt and in the solid state. Widely different views continue to be expressed in the literature ranging from liquid–liquid phase segregation[22] to complete homogeneity in the melt[23] for mixtures of high-density (HDPE) and low-density (LDPE) polyethylenes. An obvious way to distinguish between these options is to perform SANS experiments, which were attempted over a decade ago, though the analysis was inconclusive due to some puzzling features which were not understood at the time. For example, SANS from 50/50 mixtures indicated that the components were compatible in the melt when only part of the HDPE was D-labeled. However, if all of the HDPE was deuterated, the system apparently phase separated.

As a result of the research presented in this paper, such behavior can now be understood as resulting from the isotopic interaction parameter ($\chi_{HD} \sim 4 \times 10^{-4}$) between labeled and unlabeled C_2H_4 segments. Because the number of units on the chains (N) was large enough to exceed the critical condition for demixing ($N\chi_{HD} = 2$), phase segregation at higher labeling levels was an artifact caused by isotope effects rather than a basic incompatibility between the (unlabeled) species. Recent experiments[24] with components of lower molecular weight (and hence lower N) ensure that $N\chi < 2$ and demonstrate that HDPE/LDPE mixtures are compatible in the melt for all compositions. Along with studies of the effect of branching on thermodynamic interactions in polyolefins,[25–27] this work provides an essential background for SANS experiments designed to probe the thermodynamics of blends of HDPE and LDPE with polyolefins with different types of branching (e.g., linear low-density polyethylene).

Experimental Section

Sample Preparation. (1) Polyethylene. Twenty-five grams ($M_w \simeq 110\,000$; $M_w/M_n \simeq 3.7$) of 98% deuterated PE (DPE) was purchased from MSD Isotopes and subjected to a fractionation procedure to obtain narrow molecular weight (MW) samples. Polyethylene sample details are shown in Table 1.

Table 2. Polystyrene Sample Details

N_D	M_w/M_n	N_N	M_w/M_n	ϕ_D
11 500	1.3	15 400	1.1	0.050, 0.100, 0.307
11 500	1.3	8 700	1.1	0.125, 0.25, 0.375, 0.50, 0.627, 0.70, 0.875

Fractionations were conducted in cylindrical columns measuring 1.5 m in height and 5.2 cm in diameter, packed with 0.2-mm glass beads. Ethylene glycol was circulated through a jacket surrounding each column for precise temperature control. The parent polymer was dissolved in a solution of 75% 1,2,4-trimethylbenzene (TMB) and 25% butylcellosolve (BCS) at 130 °C. Solutions were allowed to drain into the columns, which were then cooled to room temperature ($\simeq$0.6 °C h^{-1}), allowing for deposition of the polymer on the silica support and facilitating a layering of molecular weights on the substrate, with the less soluble, higher molecular weight material precipitating first.

Once deposited, initial fractions were obtained using "temperature rising elution fractionation" (TREF)[28] which discriminates on the basis of dissolution temperature and, therefore, as we have verified in the absence of branching, on the basis of MW, as crystallite melting temperature increases with MW.[29] The temperature of the column was increased in steps from room temperature to 130 °C. At each step the column was filled with solvent, and after equilibration ($\simeq$20 h), the solution in the column was displaced by fresh BCS (a poor PE solvent). At 130 °C the column was eluted with varying solvent/nonsolvent (BCS/TMB) mixtures to yield increasingly higher MW fractions.[30] To extract the polymer out of solution, acetone was used as a precipitant, followed by filtering and vacuum drying. A total of 52 fractions (1/day) was obtained in the range 3K $\leq$ MW $\leq$ 500K. For MW < 200K polydispersities were $1.1 \leq M_w/M_n \leq 1.5$, while for MW > 200K, $1.5 < M_w/M_n < 1.4$.

The protonated PE (HPE), furnished by the Research and Development Division of the Phillips Petroleum Co., were synthesized under conditions known to yield a broad MW homopolymer (Ti-based catalyst) and fractionated using the above procedure. No branching was detected by NMR in this material.

Blends were prepared by codissolving the HPE and DPE at 130 °C in 75% TMB/25% BCS, followed by quenching in acetone at room temperature, filtering, and vacuum drying. All solvents employed in blending and fractionation steps contained an antioxidant package (a 50/50 mixture of Irgafos 168 and Toponol) to inhibit thermal degradation, of which none was detected in a set of tests.

Molecular weight averages and distributions were determined by gel permeation chromatography (GPC) using a Waters Model 150 CV. Instrument calibration was provided by a broad distribution PE standard (Marlex 5003) which was, in turn, characterized by light scattering measurements and comparison with NBS 1475 standard.

Of importance for the SANS measurements is the production of samples with a minimum of voids, as the scattering length density difference between small voids ($\sim$100 Å) and matrix generates an extra scattering signal, which must be subtracted from the data. In order to minimize the errors associated with this correction, the material was inserted in a brass die, pressed with a 1 kg mass, and put in a vacuum oven at 160 °C (0.7 Pa) for 2 h. This resulted in samples of 15 mm in diameter with a thickness of ca. 0.6 mm, with a minimum of void scattering (see below).

(2) Polystyrene. Monodisperse atactic (anionic) polystyrenes were obtained from Pressure Chemical Co., and the degrees of polymerization are listed in Table 2. Binary mixtures ($\sim$0.1-mm-thick films) containing a range of concentrations ($0.05 < \phi_D < 0.886$) of perdeuterated (>99% d_8) and normal (protonated) polystyrenes were prepared by solvent casting from toluene solution (<1% w/w) containing both polymer components, followed by vacuum drying at 130 °C. Stacks of solvent-cast films were subsequently pressure-molded (5 MPa) under vacuum (<1.4 Pa) into approximately 1-mm-thick samples. Molding was conducted for 12 h at 200 °C, followed by annealing for 12 h at 160 °C and quenching (<3 s). Some samples were also annealed at other temperatures in the range 138–215 °C and quenched to

room temperature before measuring $\chi_{HD}(T)$. This procedure provides sufficient time for the establishment of equilibrium composition fluctuations at the annealing temperature and "freezes" the structure of the melt into the glassy state.

The initial purpose of these studies was to establish the existence of a finite (positive) χ_{HD} for polystyrene. We have therefore repeated and extended the earlier data[2] to give the detailed concentration dependence and performed several cross-checks. In view of the time interval between the current and previous measurements, some of the samples were rerun at room temperature and also at 160 °C. SANS measurements indicated that none of the samples had aged, and comparisons of the 23 and 160 °C data showed that the quenched samples gave a true indication of the melt thermodynamics (see below).

SANS Measurements. The data were collected on the W. C. Koehler 30-m SANS facility[31] at the Oak Ridge National Laboratory (ORNL) via a 64 × 64 cm² area detector with cell (element) size ~1 cm² and a neutron wavelength (λ) 4.75 Å. The detector was placed at sample–detector distances in the range of 14–19 m, and the data were corrected for instrumental backgrounds and detector efficiency on a cell-by-cell basis prior to radial averaging, to give a Q-range of $0.003 < Q = 4\pi\lambda^{-1} \sin\theta < 0.04$ Å^{-1}, where 2θ is the angle of scatter. The coherent intensities of the sample were obtained by subtracting the intensities of the corresponding sample cells with quartz windows, which formed only a minor correction (<5%) to the sample data. The net intensities were converted to an absolute (±4%) differential cross section per unit sample volume [$(d\Sigma/d\Omega)(Q)$ in units of cm^{-1}] by comparison with precalibrated secondary standards, based on the measurement of beam flux, vanadium incoherent cross section, the scattering from water, and other reference materials.[32]

The detector efficiency calibration was based on the scattering from light water, and this led to angle-independent scattering for vanadium, H-polymer blanks, and water samples of different thicknesses in the range of 1–10 mm. The cross sections of various unlabeled (PEH, PSH) and fully labeled (PED, PSD) blanks were also measured as a basis for subtracting the coherent and incoherent backgrounds. The former arises principally from residual void scattering at low Q and is negligible for $Q > 0.007$ Å^{-1}. The latter is a flat background (~0.1–0.6 cm^{-1}), due to the H^1 incoherent cross section (σ ~80 × 10^{-24} cm²) and may be subtracted via empirical methods.[34]

The samples were contained between two 1-mm quartz plates (transmission = 0.95). The temperature and sample position of a four-position furnace were controlled via IEEE-488 interface from the system's computer. The temperature stability of the furnace and the accuracy of temperature measurement were within ±1 °C. Except where indicated, all PE runs were taken at 140 °C or higher temperature, and the PS runs were taken at room temperature. The sample transmission was measured as described previously,[24] and, in principle, this quantity is a function of temperature, due to the change of the H^1 incoherent cross section.[33] In practice, the transmission of a 1-mm-thick sample of a 50/50 blend varied by <1% between room temperature and 200 °C, because the increasing incoherent cross section of H^1 is offset by the decreasing density of the polymer.

Data Treatment. To correct the data for the effect of voids in the samples, the (flat) incoherent background was first removed[34] and then a portion of the Q-dependent scattering from a deuterated blank was subtracted from each dataset.[34] This correction is based on the assumption that void scattering is the same in the blank and blend samples. In general, the corrections for incoherent scattering[34] produce negligible error at all Q-values and coherent corrections are negligible for $Q > 0.01$ Å^{-1}. This is indicated in Figure 1, which shows typical cross sections of 50/50 labeled samples and 100% D- and H-blanks. For a blend with ϕ_D ~0.5, a fraction (~23% for PE and ~50% for PS) of the D-blank cross section is subtracted;[34] this correction is 1–2 orders of magnitude less than the sample signal. However, for low ($\phi_D < 0.15$) or high ($\phi_D > 0.85$) levels of D-labeling, the correction was a larger fraction of the data, since the coherent signal is proportional to $\phi_H\phi_D$. The correction was especially large for predominantly deuterated samples; for example, ≃90% of the D-blank cross section was subtracted from data of samples

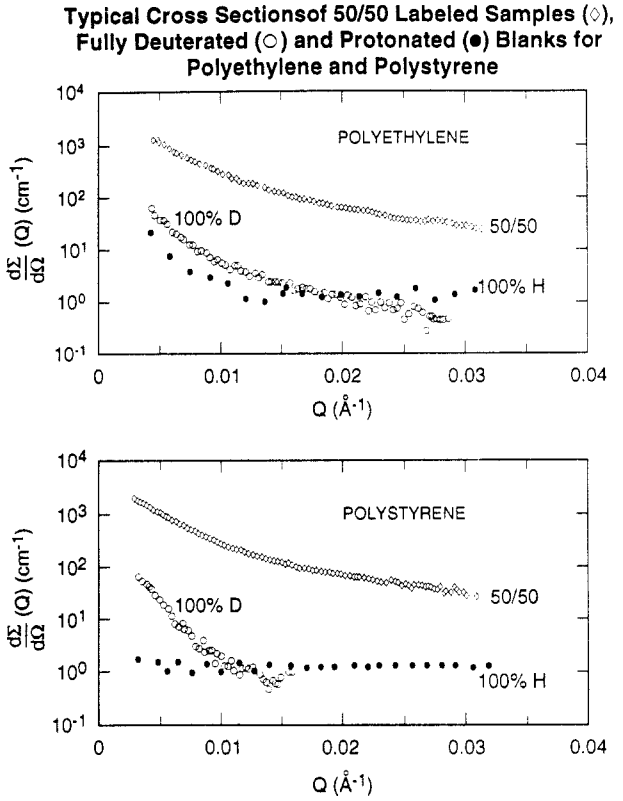

Figure 1. Typical cross sections of 50/50 labeled samples and fully deuterated and protonated blanks for polyethylene and polystyrene.

with $\phi_D \simeq 0.9$. Particular care was needed in subtracting the background for these samples, and the resultant error was larger (see below).

The corrected cross sections $(d\Sigma/d\Omega)(Q)$ are related to the static structure factor, $S(Q)$, by

$$\frac{d\Sigma}{d\Omega}(Q) = \frac{(a_H - a_D)^2}{V} S(Q) \tag{1}$$

where

$$a = \sum_i b_i \tag{2}$$

and b_i is the scattering length of atom i, an index which runs over the atoms in a segment (repeat unit) of PE (C_2H_4 or C_2D_4) or PS (C_8H_8 or C_8D_8). The segment volume (V) was assumed to be the same for both isotopic species and was calculated from the known variation of $\rho(T)$ for PE[35] and PS.[36] The data were fitted via the random phase approximation[37] (RPA) expression

$$\frac{1}{S(Q)} = \frac{1}{N_D\phi_D g_D(x)} + \frac{1}{N_H(1-\phi_D)g_H(x)} - 2\chi \tag{3}$$

The single-chain structure function was assumed to be of the Debye form,

$$g(x) = (2/x^2)[x - 1 + e^{-x}] \tag{4}$$

$$x = R_g^2 Q^2 \tag{5}$$

$$R_g^2 = Na^2/6 \tag{6}$$

where R_g and N are the radius of gyration and degree of polymerization of the molecules. The segment length (a) was assumed to be the same for both components, as expected for isotopic blends.

As discussed previously by Bates and co-workers,[13] the data at the lowest Q-values are sensitive to χ but relatively unaffected by changes in the segment length (a). As the latter parameter

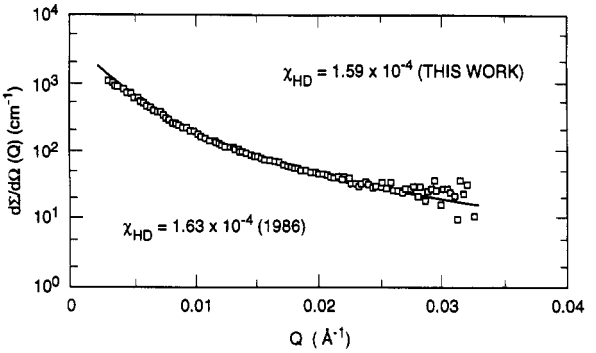

Figure 2. Fit to the RPA for a mixture of PSD (ϕ_D = 0.2, N_D = 11 500) and PSH (ϕ_H = 0.8, N_H = 15 400) quenched to T = 23 °C from T = 160 °C.

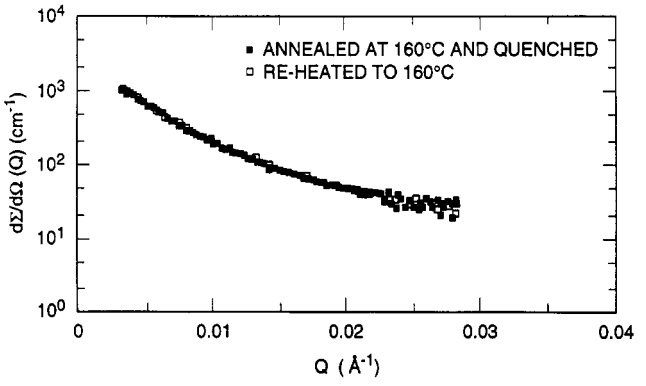

Figure 3. (dΣ/dΩ)(Q) vs Q for a mixture of PSD (ϕ = 0.2) and PSH (ϕ = 0.8) measured at 160 °C and also at 23 °C (after quenching).

is well established in the literature, the most accurate determination of the interaction parameter is achieved by fixing the segment length and fitting the data to the RPA with only one adjustable parameter (χ). For polystyrene, the literature values[2,14,38] can be summarized as $R_g = 0.27M_w^{0.5} = a(N/6)^{0.5}$, with a = 6.74 ● 0.1 Å, and are known[38] to be virtually independent of temperature in the range of 140–215 °C. Figure 2 shows the RPA fit for a sample (ϕ_D = 0.2, N_D = 11 500; ϕ_H = 0.8, N_H = 15 400) annealed at 160 °C and quenched to the glassy state. The fitted value, $\chi_{HD} = 1.59 \times 10^{-4}$ is close to the previously measured value[2] ($\chi_{HD} = 1.63 \times 10^{-4}$), indicating that the sample had not aged. Evidence that the composition fluctuations generated in the melt were truly "arrested" on quenching is given in Figure 3, which shows that data from a quenched sample and from a sample at temperature (T = 160 °C) are virtually identical.

For polyethylene, the segment length is known[38] to be temperature dependent, and two strategies were explored in the data analysis. First, the data were fitted with two adjustable parameters (a and χ_{HD}), and the results were compared with independent determinations of a, the statistical segment length. This led to a range of segment lengths (e.g., 5.69–6.43 Å at 140 °C) as a function of N and ϕ. The average (a = 5.97 Å) is within 0.5% of independent values[38-40] summarized[14,39,40] as $R_g = 0.46M_w^{0.5} = a(N/6)^{0.5}$. Moreover, the values of the segment length, obtained in the two parameter fits, were used to determine the temperature dependence of this quantity, $a(T)$. This led to a value of the thermal coefficient of expansion $\kappa = d(\ln R_g^2)/dT = (-1.1 \pm 0.1) \times 10^{-3}$ K^{-1}, compared to independent determinations of (−1.07 ± 0.08) × 10^{-3} K^{-1} and (−1.24 ± 0.06) × 10^{-3} K^{-1} via SANS.[39] In view of the excellent agreement with independent literature citations, a second strategy of data analysis was followed. Only χ_{HD} was allowed to vary (as in the case of polystyrene), while the segment length was fixed independently via eq 7

$$a(T) = 5.97 \exp\left[\frac{\kappa(T-T_0)}{2}\right] \quad (7)$$

where $\kappa = -1.1 \times 10^{-3}$ and T_0 = 140 °C. The comparison of fitted and calculated (via eq 7) values of the segment length showed that all of the fitted values were symmetrically scattered (±3%)

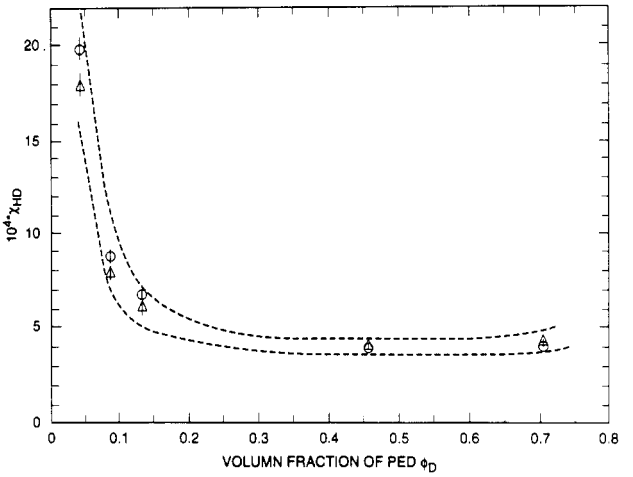

Figure 4. χ_{HD} vs ϕ_D for polyethylene isotopic blends (N = 4400) at 170 °C. (Δ) Two-parameter fit. (O) One-parameter fit. (- - -) Error limits in χ_{HD} due to systematic errors in N and absolute calibration.

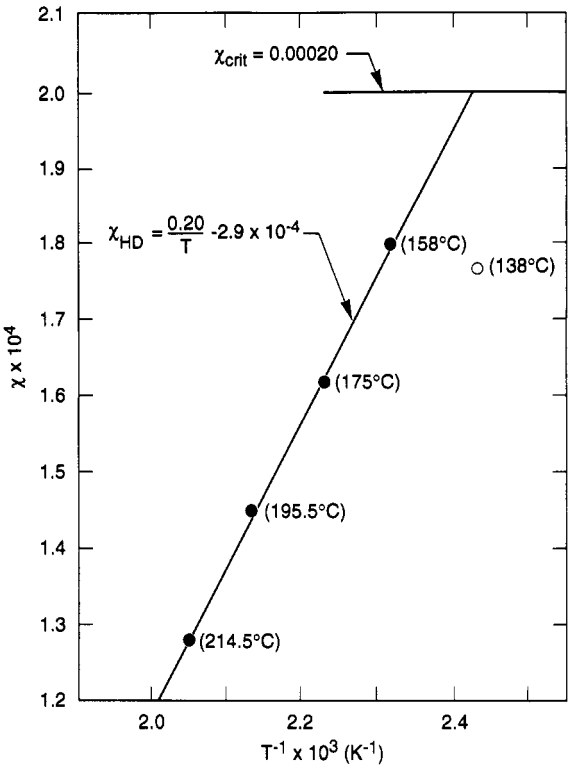

Figure 5. χ_{HD} versus T^{-1} for isotopic polystyrene mixtures.

about the calculated values. The differences in the values of χ_{HD}, obtained via the two data analysis strategies, are illustrated in Figure 4. The values of $\Delta\chi/\chi$ were less than 10% for most of the samples.

Results and Discussion

Figure 5 shows the temperature dependence of $\chi(T)$, over the range 158 < T < 215 °C, for the sample of PSD (ϕ_D = 0.5; N_D = 8700) and PSH (N_H = 15 400). The result may be expressed as

$$\chi_{HD} = A/T + B \quad (8)$$

with A = 0.20 K and $B = -2.9 \times 10^{-4}$. Samples annealed at lower temperatures did not reach equilibrium in the 12-h annealing time, due to the proximity of the glass transition as indicated by the sample annealed at 138 °C (Figure 5).

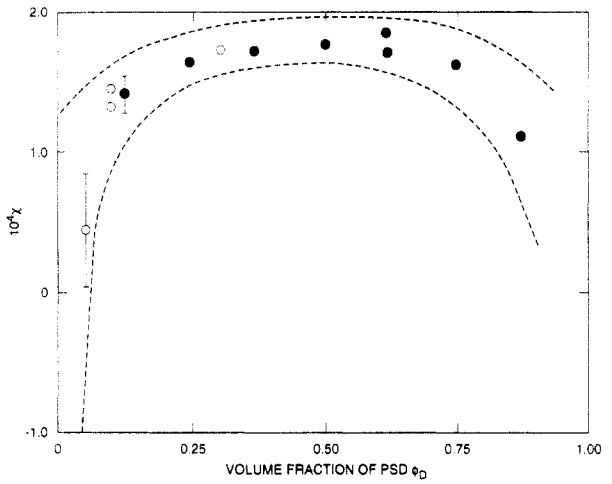

Figure 6. χ_{HD} vs ϕ_D for polystyrene (PSH/PSD) blends at 160 °C. (●) $N_H = 8700/N_D = 11\,500$. (○) $N_H = 15\,400/N_D = 11\,500$. (- - -) Error limits in χ_{HD} due to systematic errors in N and absolute calibration.

Figure 6 shows the concentration dependence of χ_{HD} at $T = 160$ °C. In contrast to PVE and PEE,[1] the interaction parameter shows a maximum at $\phi \simeq 0.5$, suggesting that the details of the chain architecture and packing can influence the basic interaction caused by differences in volume and polarizability between labeled and unlabeled segments. Schwahn and co-workers[21] have also studied isotopic PS mixtures and observed a maximum in the concentration dependence of χ_{HD}, though their SANS-determined interaction parameter (Γ) was observed to be *negative* for $\phi_D > 0.8$ and $\phi_D < 0.2$. To our knowledge, all previous experimental determinations[1-3,14,26,27,41-44] and theoretical estimates[12,13,45] of the isotopic interaction parameters have been positive, and we are unaware of any mechanism which could change the sign of this quantity. However, as noted previously, the errors involved in determining χ_{HD} are greatest at low ($\phi_D < 0.2$) and high ($\phi_D > 0.8$) concentrations, where the coherent signal (which is proportional to $\phi_H\phi_D$) is smallest.

In view of the fact that PS has a different functional form to all previous measurements of $\chi(\phi)$, it is important to establish that the observed variation is within the experimental error, especially in the wings where the uncertainties are greatest. This may be accomplished by estimating the effects of random and systematic errors on χ_{HD}, and a full error analysis is given in Appendix 1. The error bars in Figure 6 represent the maximum uncertainties in $\chi_{HD}(\phi)$ with respect to *random* errors in the transmission (±1.3%), thickness (±2.0%), volume fraction ϕ (±0.5%), and counting statistics (±0.2%). The dotted envelope represents the maximum error limits due to possible *systematic* errors in the absolute calibration procedures (±3.5%), the segment length, a (±2.0%), and the degree of polymerization, N (±5.0%). In addition, systematic errors also arise in connection with the substraction of the coherent background, though these are virtually negligible for $0.2 < \phi_D < 0.8$. It may be seen that no combination of the estimated random and systematic errors could change the observed variation into a parabolic upward dependence. Even if all the errors combined in such a fortuitous manner as to reduce the functional dependence of $\chi(\phi)$, then at most the curve might be flattened out. In order to change the functional form, we believe that the error in N would have to approach 10–15%. We believe that the possibility of such a scenario is remote and that $\chi_{HD}(\phi)$ has the functional dependence indicated in Figure 6. However, the combination of systematic and random errors could plausibly account for the negative values observed in the wings by Schwahn et al.[21] as discussed above, we know of no mechanism that could otherwise change the sign of this parameter.

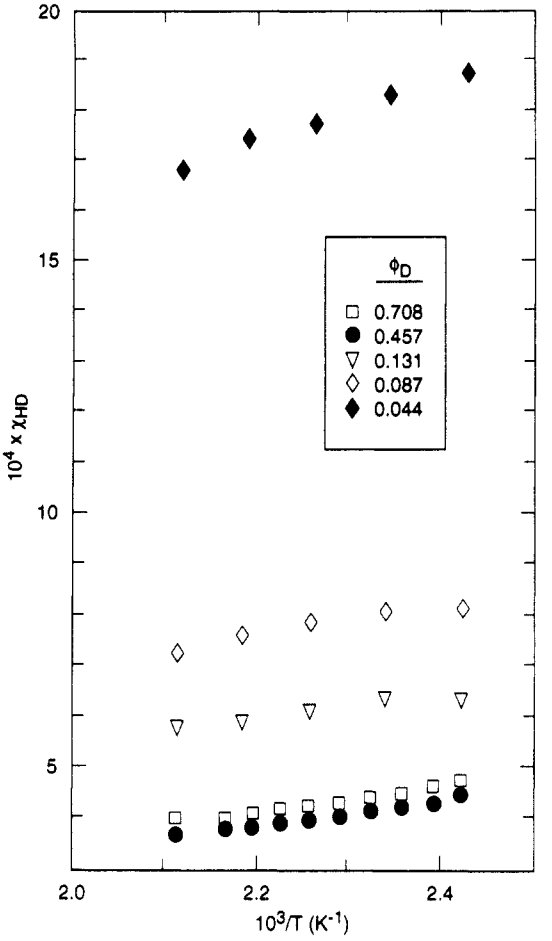

Figure 7. χ_{HD} vs T^{-1} and ϕ_D for polyethylene isotopic blends (N = 4400).

For PE, the error analysis is not as essential as for PS, because the functional dependence of $\chi_{HD}(\phi)$ is much stronger. Also, there is no conceivable combination of random or systematic errors that could change the sign of χ_{HD}, the observed parabolic upward dependence, or the trends as a function of N. However, for the sake of completeness, we have added random and systematic errors limits based on the same potential uncertainties as for PS and these are indicated in Figure 4.

Figure 7 shows that, for PE, $\chi_{HD}(T)$ also shows a linear temperature dependence with T^{-1} (eq 8). Table 1 shows the results of the fits to eq 8. As shown in Figure 7, the slope (A) is independent of ϕ to a good approximation, with an average value $A = 0.14$. In contrast, B is strongly composition-dependent (Figure 8), and this variation is the main cause of the parabolic upward composition dependence of χ_{HD}. Thus the concentration dependence of the interaction parameter for PE (Figure 8) appears to arise from the temperature-independent term, reflecting the effects of noncombinatorial entropy.

Figure 8 shows that χ_{HD} and the curvature of its parabolic upward composition dependence decrease with an increase in the chain length. Measurements on structurally asymmetric[45] and isotopic[1] blends exhibit a similar behavior. The numerical calculations of Yethiraj and Schweizer[46] for symmetric blends of long chains follow qualitatively the same trends as presented here for PE. In contrast, numerical results[20] from shorter chains ($N < 250$) follow the opposite trend; i.e., the composition dependence

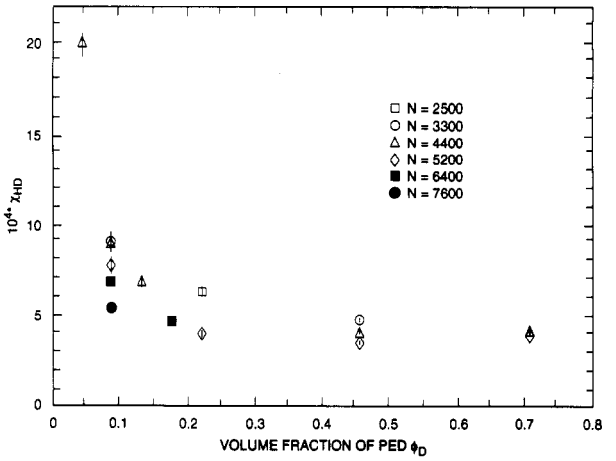

Figure 8. χ_{HD} vs ϕ_D and N for polyethylene isotopic blends at 170 °C.

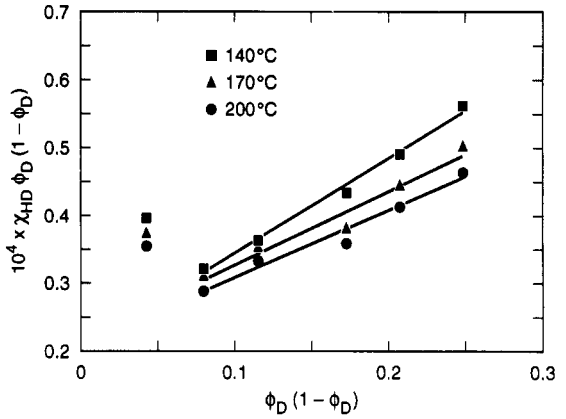

Figure 9. Plot of $\chi_{HD}\phi_D(1 - \phi_D)$ vs $\phi_D(1 - \phi_D)$ for polyethylene (N = 4400).

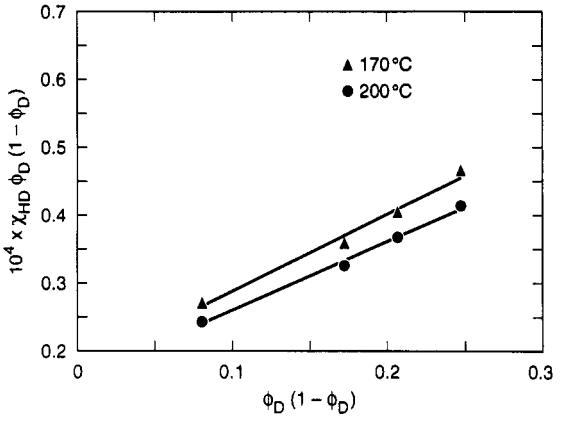

Figure 10. Plot of $\chi_{HD}\phi_D(1 - \phi_D)$ vs $\phi_D(1 - \phi_D)$ for polyethylene (N = 5200).

becomes more pronounced with an increase in N.

Krishnamoorti et al.[19] have obtained reasonable fits to SANS data from several isotopic systems with an empirical relationship (eq 9), which was fitted to the χ_{HD} values for PE as shown in Figures 9 and 10.

$$\chi\phi_D(1 - \phi_D) = \beta\phi_D(1 - \phi_D) + \gamma \quad (9)$$

The points at the lowest values of ϕ_D in Figure 9 have large error bars and were therefore not included in the fits. Figure 11 shows that β decreases with increasing temperature and that β appears to be MW-independent. Figure 12 shows that γ appears to be independent of temperature while it decreases with an increase in MW. This is in agreement with observations based on the data

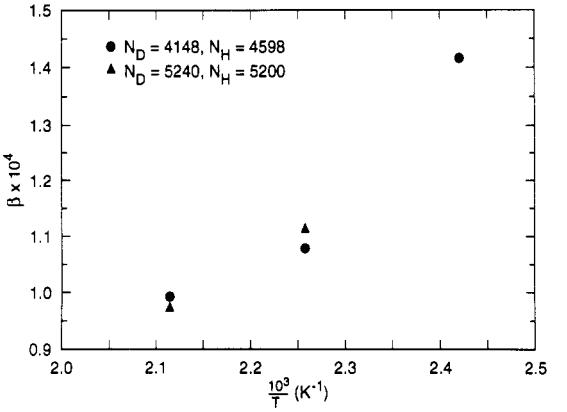

Figure 11. Plot of β vs $1/T$.

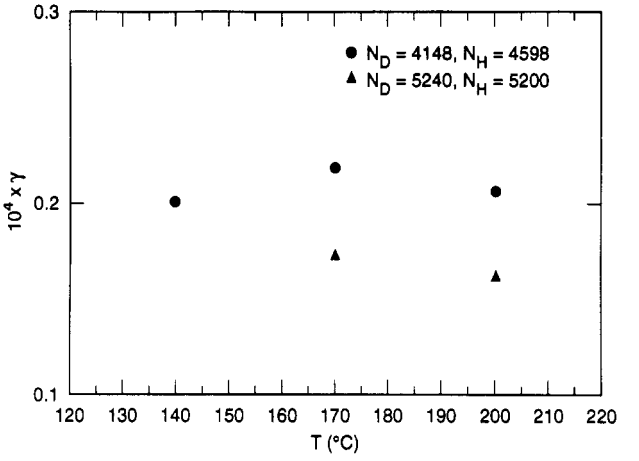

Figure 12. Plot of γ vs T.

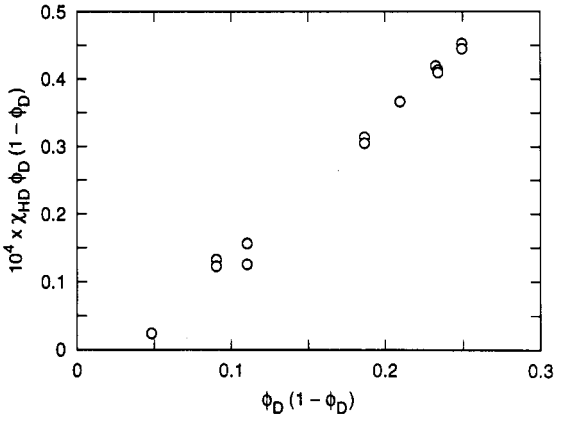

Figure 13. Plot of $\chi_{HD}\phi_D(1 - \phi_D)$ vs $\phi_D(1 - \phi_D)$ for polystyrene isotopic blends.

shown in Figure 8; see above. The value of the parameter γ increases with the curvature of the parabolic upward composition dependence. More comprehensive studies are needed to probe these trends in detail and to determine the precise degree of agreement with eq 9.

Figure 13 shows that the PS data obeys the empirical relationship (eq 9) to a good approximation. The data indicate that χ_{HD} is positive over virtually the whole concentration range and should only change sign close to the extremities (ϕ_D or $\phi_H < 0.03$). In view of the increased experimental uncertainties in the wings, however, we believe that apparent crossover at $\phi \sim 0.03$ is within the experimental error. A negative χ_{HD} is inconsistent with the repulsive interactions known to exist between the species in an isotopic blend as discussed above.

As mentioned earlier, these data throw light on previous[47] and recent[24] SANS experiments and on the state

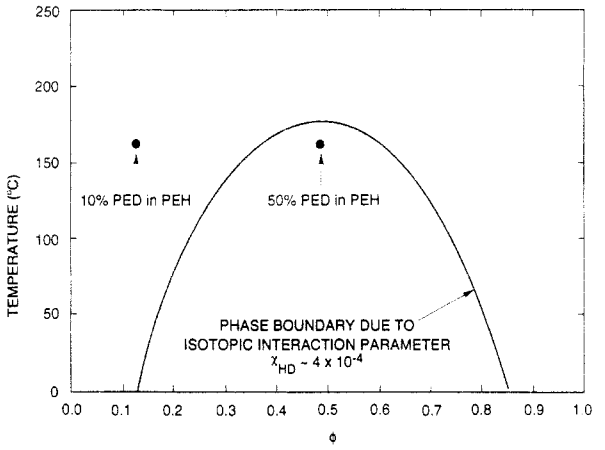

Figure 14. Phase diagram of isotopic mixtures of linear protonated (PEH) and deuterated (PED) polyethylenes (N_H = N_D = 5200).

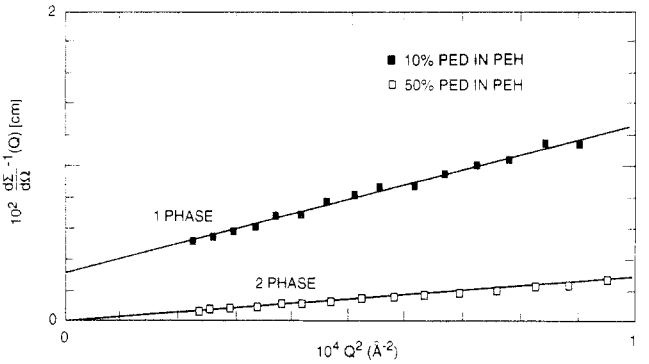

Figure 15. Ornstein–Zernicke plots for mixtures of linear PEH and PED.

of mixing in blends of linear (high-density) and branched (low-density) polyethylenes. In the previous work[47] it was observed that SANS experiments on 50/50 mixtures of HDPE/LDPE indicated that the components were compatible in the melt when only part of the HDPE was deuterium-labeled. However, if all of the HDPE was deuterated, the system apparently phase separated. Figures 14 and 15 illustrate how such effects arise, even in linear/linear blends with no thermodynamic interactions other than isotope effects. The phase boundary arises from the isotopic interaction parameter ($\chi_{HD} \sim 4 \times 10^{-4}$) between the labeled ($C_2D_4$) and unlabeled ($C_2H_4$) segments. While the 50/50 blend is within the two-phase region in Figure 15, the opposite is true for the 10/90 blend. The Ornstein–Zernicke plots in Figure 15 confirm this assertion, giving a positive intercept for the 10PED/90PEH blend, as expected for homogeneous systems. Alternatively, for the 50PED/50PEH system, the intercept is negative as expected for phase-separated blends. Such behavior is independent of the branching of the blend components but dependent on the degree of polymerization (N) or MW. In actual fact, this blend is completely homogeneous in the absence of isotope effects, though different conclusions concerning the phase stability could be drawn if this artifact was not accounted for.

Acknowledgment. We gratefully acknowledge M. Hildebrand, J. R. Donaldson, E. A. Robles, D. J. Henson, J. D. Wood, and B. E. Jones of the Phillips Petroleum Co. for their technical assistance in preparing and characterizing the samples. Research was supported in part by the Division of Materials Sciences, Office of Basic Energy Sciences, U.S. Department of Energy under Contract No. DE-AC05-840R21400 with Martin Marietta Energy Systems Inc.

Appendix 1. Error Analysis

Equation 3 can be expressed as

$$\chi_{HD} = \frac{1}{2}\left(\frac{1}{S_{id}} - \frac{1}{S(Q)}\right) \tag{A1}$$

If $N_D = N_H = N$ and $g_H = g_D = g$, then

$$S_{id} = Ng(x)\,\phi_d(1-\phi_d) \tag{A2}$$

also[32]

$$S(Q) = \left(\frac{I(Q)r^2}{tTK_NA}\right)\left(\frac{V}{(a_H - a_D)^2}\right) \tag{A3}$$

Some of the quantities which appear in eqs A2 and A3 were used unchanged in all determinations of χ_{HD}. Changes in these quantities would shift all values of χ_{HD} in the same sense, and their uncertainties lead to systematic errors. Other quantities, like thicknesses and transmissions, varied from sample to sample. Changes in these quantities do not necessarily shift all values in the same sense and affect, more readily than systematic errors, the relative differences between values of χ_{HD}; uncertainties in these quantities lead to random errors. Therefore, systematic and random sources of error can be identified. Fractional standard errors (fse) for the quantities which led to random errors in χ_{HD} in eqs A2 and A3 were 2% in t (sample thickness), 1.3% in T (sample transmission), 0.5% in ϕ_D (volume fraction of deuterated component), and 0.2% in $I(Q)$ (neutron intensity in counts per second). For the quantities which led to systematic errors, the fse were 5% in N (degree of polymerization), 2% in a (statistical segment length), 0.05% in scattering lengths, 0.2% in density, and 4.0% in the absolute intensity constant, which groups together the beam flux, distance from sample to detector (r), sample area (A), detector efficiency etc.[28] In the case of N, we have neglected all contributions from random errors in N. We assume χ_{HD} to be a function of a set of measured quantities, m_i, with standard errors σ_i. Since $g(x)$ in eq A1 is a function of Q, we can calculate a Q-dependent error in χ_{HD} from[48]

$$\sigma_{\chi_{HD}}{}^2(Q) = \sum_i \left(\frac{\partial \chi_{HD}}{\partial m_i}\right)^2 \sigma_i{}^2 \tag{A4}$$

which leads, for example, to the following expression for the fse in $S(Q)$ due to random errors.

$$\left(\frac{\sigma_{S(Q)}}{S(Q)}\right)_r^2 = \left(\frac{\sigma_t}{t}\right)^2 + \left(\frac{\sigma_T}{T}\right)^2 + \left(\frac{\sigma_{I(Q)}}{I(Q)}\right)^2 \tag{A5}$$

The fse of $I(Q)$ was taken to be uniform over Q. Equation A4 also leads to the following expression for the fse in S_{id} due to systematic errors,

$$\left\{\frac{\sigma_{S_{id}}}{S_{id}}(Q)\right\}_s^2 = \left(\frac{\sigma_N}{N}\right)^2 + \left(\frac{\sigma_{g(x)}}{g(x)}\right)^2 \tag{A6}$$

A final value for $\sigma_{\chi_{HD}}$ was estimated from the following expression for the weighted average of the set of $\sigma_{\chi_{HD}}(Q)$:

$$\sigma_{\chi_{HD}} = \frac{\sum (S(Q) - S_{id})\sigma_{\chi_{HD}}(Q)}{\sum (S(Q) - S_{id})} \tag{A7}$$

References and Notes

(1) Bates, F. S.; Muthukumar, M.; Wignall, G. D.; Fetters, L. J. *J. Chem. Phys.* **1988**, *89*, 535. Muthukumar's theory predicts a

parabolic upward behavior (the last term in eq 11 in the paper by Bates et al.[1] should be negative: Muthukumar, M., private communication).
(2) Bates, F. S.; Wignall, G. D. *Macromolecules* **1986**, *19*, 932.
(3) Bates, F. S.; Wignall, G. D.; Koehler, W. C. *Phys. Rev. Lett.* **1985**, *55*, 2425. Bates, F. S.; Wignall, G. D. *Phys. Rev. Lett.* **1986**, *57*, 1429.
(4) Wignall, G. D.; Bates, F. S. *Makromol. Chem.* **1988**, *15*, 105.
(5) Flory, P. J. *Discuss. Faraday Soc.* **1986**, *64*, 2035.
(6) Sanchez, I. C.; Lacombe, R. H. *J. Phys. Chem.* **1976**, *80*, 2352. Lacombe, R. H.; Sanchez, I. C. *J. Phys. Chem.* **1976**, *80*, 2568. Walsh, D. J.; Rostami, S. *Adv. Polym. Sci.* **1985**, *70*, 119.
(7) Freed, K. F.; Pesci, A. I. *J. Chem. Phys.* **1987**, *87*, 7342. Pesci, A. I.; Freed, K. F. *J. Chem. Phys.* **1989**, *90*, 2003 and 2017.
(8) Bawendi, M. G.; Freed, K. F. *J. Chem. Phys.* **1988**, *88*, 2741. Freed, K. F.; Bawendi, M. G. *J. Phys. Chem.* **1989**, *93*, 2194. Tang, H.; Freed, K. F. *Macromolecules* **1991**, *24*, 958.
(9) Dudowicz, J.; Freed, M. S.; Freed, K. F. *Macromolecules* **1991**, *24*, 5096. Dudowicz, J.; Freed, K. F. *Macromolecules* **1991**, *24*, 5076 and 5112; *Macromolecules* **1990**, *23*, 1519; *J. Chem. Phys.* **1992**, *96*, 9147. Freed, K. F.; Dudowicz, J. *J. Chem. Phys.* **1992**, *97*, 2105.
(10) Banaszak, M.; Petsche, I. B.; Radosz, M. *Macromolecules* **1993**, *26*, 391.
(11) Schweizer, K. S.; Curro, J. *Phys. Rev. Lett.* **1988**, *60*, 809.
(12) Buckingham, A. B.; Hentschel, H. G. E. *J. Polym. Sci., Polym. Phys. Ed.* **1984**, *18*, 853.
(13) Bates, F. S.; Wignall, G. D. *Phys. Rev. Lett.* **1986**, *57*, 1429. Bates, F. S.; Fetters, L. J.; Wignall, G. D. *Macromolecules* **1988**, *21*, 1086.
(14) Wignall, G. D. *Encycl. Polym. Sci. Eng.* **1987**, *10*, 112.
(15) Gehlsen, M. D.; Rosedale, J. H.; Bates, F. S.; Wignall, G. D.; Hansen, L.; Almdal, K. *Phys. Rev. Lett.* **1992**, *68*, 2452.
(16) Deutsch, H. P.; Binder, K. *Europhys. Lett.* **1992**, *17*, 697.
(17) Yethiraj, A.; Schweizer, K. *J. Chem. Phys.* **1992**, *97*, 5927.
(18) Sariban, A.; Binder, K. *J. Chem. Phys.* **1987**, *86*, 5859; *Colloid Polym. Sci.* **1989**, *267*, 469; *Macromolecules* **1988**, *21*, 711; *Makromol. Chem.* **1988**, *189*, 2357.
(19) Krishnamoorti, R.; Graessley, W. W.; Balsara, N. P.; Lohse, D. J. *J. Chem. Phys.*, submitted for publication.
(20) Schweizer, K.; Yethiraj, A. *J. Chem. Phys.* **1993**, *98*, 9260. Yethiraj, A.; Schweizer, K. *J. Chem. Phys.* **1993**, *98*, 9284.
(21) Schwahn, D.; Hahn, K.; Streib, J.; Springer, T. *J. Chem. Phys.* **1989**, *93*, 8383.
(22) Hill, M. J.; Barham, P. H.; Keller, A. *Polymer* **1992**, *33*, 2530.
(23) Stehling, F. S.; Wignall, G. D. *Polym. Prepr. (Am. Chem. Soc. Div. Polym. Chem.)* **1983**, *24*, 211.
(24) Alamo, R. A.; Londono, J. D.; Mandelkern, L.; Stehling, F. C.; Wignall, G. D. *Macromolecules* **1994**, *27*, 411.
(25) Graessley, W. W.; Krishnamoorti, R.; Balsara, N. P.; Fetters, L. J.; Lohse, D. J.; Schultz, D. N.; Sissano, J. A. *Macromolecules* **1993**, *26*, 1137.
(26) Nicholson, J. C.; Finerman, T.; Crist, B. *Polymer* **1990**, *31*, 2287.
(27) Rhee, J.; Crist, B. *Macromolecules* **1991**, *24*, 5663; *J. Chem. Phys.* **1993**, *98*, 4174.
(28) Wild, L. *Adv. Polym. Sci.* **1990**, *98*, 1 and references cited therein.
(29) Flory, P. J. *J. Chem. Phys.* **1947**, *15*, 684.
(30) Koningsveld, R.; Staverman, A. J. *Adv. Polym. Sci.* **1968**, *7*, 1.
(31) Koehler, W. C. *Physica (Utrecht)* **1986**, *137B*, 320.
(32) Wignall, G. D.; Bates, F. S. *J. Appl. Crystallogr.* **1986**, *20*, 28.
(33) Maconnachie, A. *Polymer* **1984**, *25*, 1068.
(34) Hayashi, H.; Flory, P. J.; Wignall, G. D. *Macromolecules* **1983**, *16*, 1328.
(35) Zoller, P. *J. Appl. Polym. Sci.* **1979**, *23*, 1051.
(36) Patnode, W.; Scheiber, W. J. *J. Am. Chem. Soc.* **1939**, *61*, 3449.
(37) de Gennes, P.-G. In *Scaling concepts in Polymer Physics*; Cornell University Press: Ithaca, NY, 1979.
(38) Boothroyd, A. T.; Rennie, A. R.; Wignall, G. D. *J. Chem. Phys.*, in press.
(39) Boothroyd, A. T.; Rennie, A. R.; Boothroyd, C. B. *Europhys. Lett.* **1991**, *15*, 715.
(40) Schelten, J.; Wignall, G. D.; Ballard, D. G. H. *Polymer* **1977**, *18*, 1111.
(41) Lapp, A.; Picot, C.; Benoit, H. *Macromolecules* **1985**, *18*, 2337.
(42) O'Connor, K.; Pochan, J. M.; Thiyagarajan, P. *Polymer* **1991**, *32*, 195.
(43) Green, P. F.; Doyle, B. L. *Phys. Rev. Lett.* **1986**, *57*, 2407.
(44) Singh, R. R.; Van Hook, W. A. *Macromolecules* **1987**, *20*, 1855.
(45) Tanaka, H.; Hashimoto, T. *Macromolecules* **1991**, *24*, 5398. Iyichi, Y.; Hashimoto, T.; Fetters, L. J. *Macromolecules* **1989**, *22*, 2817. Jung, W.; Fischer, E. W. *Makromol Chem., Macromol. Symp.* **1988**, *16*, 281.
(46) Schweizer, K. S., private communication.
(47) Stehling, F. C.; Wignall, G. D., unpublished data, 1982.
(48) Bevington, P. R. In *Data Reduction and Error Analysis for the Physical Sciences*; McGraw-Hill: New York, 1969.